PHOTONS ON A LEASH

ELECTROMAGNETICALLY INDUCED TRANSPARENCY IN SOLIDS

GIUSEPPE LA ROCCA[1], MAURIZIO ARTONI[2,3]

[1] *Scuola Normale Superiore and CNISM, Pisa*

[2] *Department of Physics and Chemistry of Materials and CNR-INFM Sensor Laboratory, University of Brescia, Brescia*

[3] *European Laboratory for Non-linear Spectroscopy (LENS), Florence*

In memory of Giuseppe Franco Bassani

Quantum coherence and interference can be used to control the light-matter interaction and the propagation of light in multilevel systems. Effects of electromagnetically induced transparency based on exciton and biexciton levels or on impurity levels in solid-state media are here reviewed. New photonic crystal structures created via coherent optical nonlinearities in such solid media are also considered and discussed.

1 Introduction

The effort to understand and control the light-matter interaction is a key issue on the materials science agenda both from the point of view of basic science and of technological applications. It has been tackled both from the side of "matter", searching for novel functional materials with improved optical properties, and from the side of "light", designing appropriate dielectric structures to mould the photon modes. As examples of the first strategy, we recall the developments in the field of semiconductor nanostructures in which the electronic properties can be engineered and in the field of organic materials in which the molecules, and to some extent the crystalline structure, can be chemically functionalized. The second line of attack has led, for instance, to the recent advances in the field of photonic crystals in which the photon modes are rearranged in bands separated by gaps just as for electrons in semiconductors, and of semiconductor microcavities which are a solid-state analogue of the atomic ones used in cavity quantum electrodynamics.

One of the major aim of these research lines is to provide systems with large all-optical nonlinearities. The capability of controlling light by light is instrumental to the development of all-optical information storage and processing techniques, including quantum computing at the single photon level. In this respect, there is usually a trade-off between the beneficial effect of the enhanced nonlinear response at resonance with specific electronic transitions and the detrimental effect of the concomitant resonant absorption. However, quantum coherence and interference effects turn out to be beneficial in circumventing this problem [1]. Three-level systems coupled to two light fields may, in fact, exhibit transparency effects that result from the cancellation of absorption at a resonant transition frequency. These effects are induced by one of the two light fields (the coupling beam) upon modifying the medium optical response to the other field (the probe beam). The large degree of transparency in a medium which would otherwise be opaque has then been termed electromagnetically induced transparency (EIT) [2].

This phenomenon has only recently been considered in solid-state media, though it has long been known in atomic systems. The spectroscopic effect that lies at the foundation of EIT, *i.e.* coherent population trapping (CPT) [3], was discovered by Gozzini's group in Pisa in the seventies when a peculiar effect, the so-called "black line", was observed in optical pumping experiments with sodium atoms. When the difference in frequency between two modes of a multimode laser happened to be equal to the separation between two Zeeman sublevels of the two 3*S* hyperfine split electronic ground states, both coupled to the same 3*P* excited state of the sodium *D*1 line, no absorption took place and hence no fluorescence off the excited state was observed. Quantum coherence was the key to such an intriguing effect as the 3*S* ground-state doublet is pumped into a coherent superposition state where the population is trapped due to destructive interference between the two distinct absorption paths to the excited 3*P* level. Long after this pioneering experiment, CPT has revived the interest of the scientific community as it lays at the heart of important phenomena such as subrecoil laser cooling, lasing without inversion and adiabatic transfer [3]. In optically dense

media, under analogous conditions as for CPT, the propagation properties of the resonant probe light itself are drastically modified leading to EIT. In particular, by using a typical three-level lambda configuration, an astonishing control on light wave propagation has been observed in sub-millimiter-sized cigar-shaped clouds of alkali atoms cooled to within a millionth of a degree above absolute zero. In such samples, group velocities as low as one meter per second and light pulse storage and retrieval have been attained, which opens the way to potential applications to all-optical quantum information processing [4].

For many potential applications, however, solid-state solutions are preferred. In such media, unfortunately, decoherence takes place rather quickly which makes the effects of electromagnetically induced transparency rather difficult to observe with respect to the atomic case, and comparatively little has been done so far in solid media. Yet, EIT effects have been observed in semiconductor quantum wells and in a class of solid materials exhibiting defect states, such as *e.g.*, presodimium-doped Y_2SiO_5 and diamond containing nitrogen-vacancy (N-V) color centers [4]. In both cases, inhomogeneous broadening plays a very significant role. Efficient solid-state solutions should rely on materials that exhibit strong light-matter interactions and little dephasings. Fairly strong optical transitions may be found in some familiar semiconductors which in turn exhibit a variety of three-level configurations in which destructive interference could be induced and whose optical response could be controlled. Narrow intrinsic resonances associated with delocalized free excitons (bound states of one electron and one hole, akin to a hydrogen atom) or exciton-polaritons (coherent superpositions of the resonant exciton and photon states mixed by the light-matter interaction) and biexcitons (bound states of two excitons, akin to a hydrogen molecule) in covalent semiconductor crystals are promising in this respect.

After a discussion of the basics of EIT, we briefly review here our own results on electromagnetically induced transparency based on intrinsic free-exciton and biexciton states as well as on color center levels in diamond. We specifically examine the case of copper oxide crystal (Cu_2O) where, akin to the atomic case, transparency may be induced through a lambda configuration obtained from the yellow series of exciton states, and the case of cuprous chloride crystal (CuCl) where a tunable transparency effect in the exciton-polariton stop band may be induced through a ladder configuration of exciton-biexciton transitions. While the former is found to be suited to investigate how EIT may be used to control light dragging in moving media and the emission of Cherenkov radiation by fast charges, the latter is most appropriate to study how the coherent control of the strong light-matter coupling regime could be achieved. Finally, we consider a scheme to realize all-optically induced photonic band gaps based on a standing wave EIT configuration which can be implemented with nitrogen-vacancy color centers in diamond. Such tunable photonic crystals are amenable to applications in optical switching, light storage and quantum nonlinear optics.

2 The basic mechanism of EIT

In the EIT regime, the cancellation of absorption relies on a process involving quantum interference between the atomic coherences in a three-level configuration, typically a lambda scheme or a ladder scheme as shown in fig.1, excited by two laser fields, the coupling beam and the probe beam, with frequencies ω_c and ω_p and Rabi

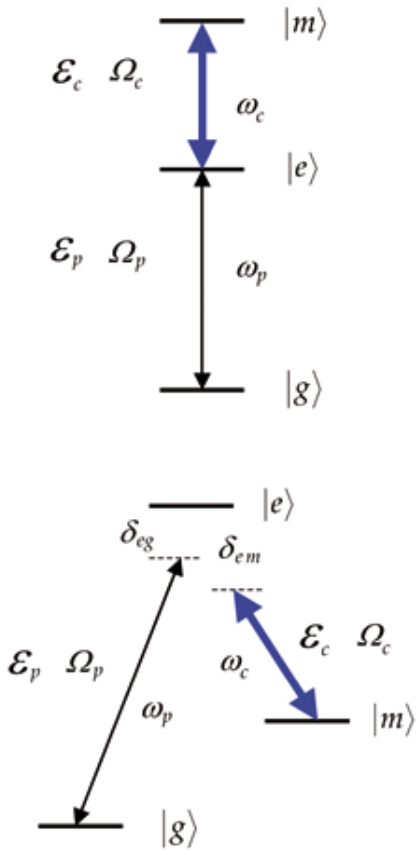

Fig. 1 Basic schemes leading to electromagnetically induced transparency (EIT). These are defined by the relative energies of the three states: (upper) a ladder (or cascade) scheme $E_g < E_e < E_m$, (lower) a lambda scheme with $E_g < E_m < E_e$. State $|m\rangle$ in the lambda scheme need not be a ground state; however, in a symmetric lambda, E_g and E_m are almost degenerate. As for coherent population trapping (CPT), the two photon (Raman) resonance condition should be met (*i.e.*, $\delta_{eg} = \delta_{em}$ in this sketch), yet the strength of one of the two applied fields could be appreciably larger than that of the other ($\Omega_p << \Omega_c$).

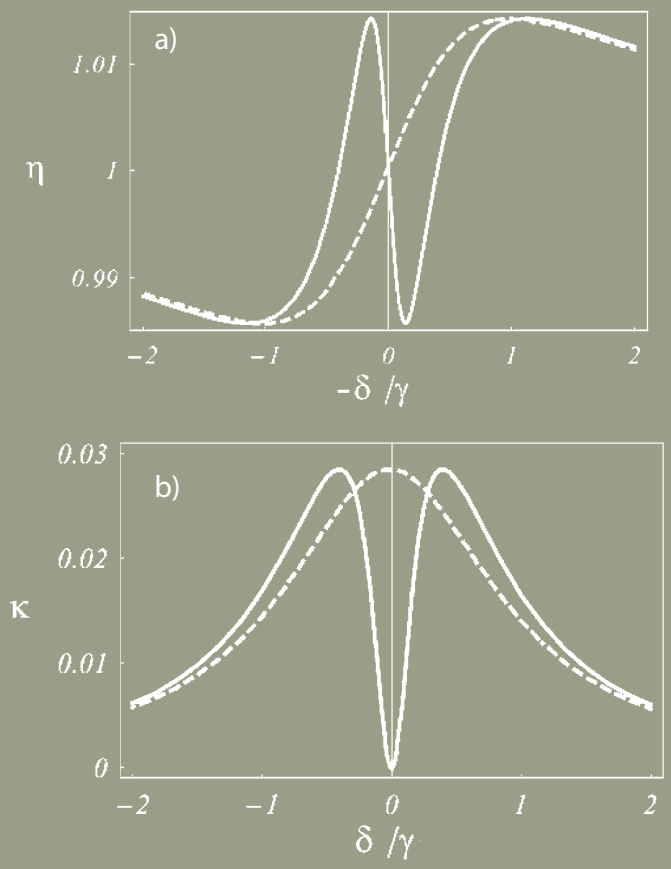

Fig. 2 Real (a) and imaginary (b) part of the probe refractive index *n* as a function of the normalized probe detuning in the absence (dashed) and in the presence (solid) of a resonant coupling beam with Rabi frequency $\Omega_c = 0.8\,\gamma$. Due to destructive interference the imaginary part κ, associated with the medium absorption, vanishes at exact resonance when the coupling field is on. The real part η, which determines the medium dispersion, is likewise modified in the presence of the coupling field and acquires a steep slope around resonance.

frequencies Ω_c and Ω_p, respectively, coupled to the e-m transition and to the e-g transitions. The Rabi frequencies are given in terms of the corresponding electric-field amplitudes and electric-dipole transition matrix elements by $\hbar\Omega_c = E_c \mu_{em}$ and $\hbar\Omega_p = E_p \mu_{eg}$. Referring to the three-level lambda scheme, the two transition amplitudes from the two lower states $|g\rangle$ (ground state) and $|m\rangle$ (metastable stable) to the common higher state $|e\rangle$ (excited state) interfere destructively if the Raman resonance condition $\hbar\,(\omega_p - \omega_c) = E_m - E_g$ is met. Most importantly, the key parameters for the occurrence of EIT are the relaxation rates and, in particular, the decay rate γ_{gm} of the coherence between the $|m\rangle$ and $|g\rangle$ states which should be small (typically a few orders of magnitude smaller than that of the optical coherence between the excited and ground level), and in this sense the state $|m\rangle$ should be metastable.
Formally coherences are identified with the off-diagonal elements of the density matrix ρ_{ij}, and most calculations on EIT effects in three-level systems are therefore developed in terms of the density matrix equations, including phenomenological relaxation terms, coupled to the propagation equations for the optical fields as given by the macroscopic Maxwell's equations [1]. Within the context of a density matrix formulation the interference that leads to induced transparency manifests itself in the vanishing of the optical coherence ρ_{eg}. This stems from the existence of the coherence ρ_{mg}, which is coupled to it and which only appears when the coupling laser beam is present. The contribution from ρ_{mg} to ρ_{eg} cancels, at the Raman resonance, with the direct contribution driving ρ_{eg} due to the applied probe field.
From an alternative theoretical viewpoint, the probability amplitude for an absorption and emission cycle contains additional terms with respect to the usual one in which the atom is first excited from $|g\rangle$ to $|e\rangle$, and then directly decays to $|g\rangle$ by spontaneous emission. In the presence of the coupling beam, additional quantum-mechanical paths are indeed available: after being excited to $|e\rangle$, the atom can emit a photon by stimulated emission to the coupling beam corresponding to a $|e\rangle$ to $|m\rangle$ transition and re-absorb it, before decaying from $|e\rangle$ back to $|g\rangle$ by spontaneous emission, or also, more photons can be coherently exchanged with the coupling beam before spontaneous decay. Summing up to all orders in the strong coupling field the amplitudes of all these paths, in Raman resonance and for appropriate parameter values, the total amplitude of the process is suppressed by destructive interference and, thus, the resonant absorption quenched.
A very useful conceptual picture is also provided by the dressed state approach: the presence of the coupling beam dresses the medium mixing states $|e\rangle$ and $|m\rangle$ so that the resonant absorption from state $|g\rangle$ no longer takes place into the bare state $|e\rangle$, but rather into a doublet of dressed states with a probability amplitude affected by quantum

interference. This leads in turn to a narrow transparency window within the resonant peak of the imaginary part of the optical susceptibility experienced by the probe, and a corresponding strong dispersion of the real part. As a matter of fact, the dressed complex susceptibility χ experienced by the probe can be written as,

$$(1)\ \chi = (|\mu_{eg}|^2 N(\delta + i\gamma_{gm})/(2\hbar\varepsilon_0 V))/[(|\Omega_c|^2/4) - (\delta + i\gamma_{gm})(\delta + i\gamma)],$$

where the coupling beam has been assumed on resonance ($\delta_{em} = 0$), the probe detuning is $\hbar\delta = \hbar\omega_p - (E_e - E_g) = -\hbar\delta_{eg}$, the decay rate of the optical coherence between the $|e\rangle$ and $|g\rangle$ states is γ and the atomic density is N/V.
The corresponding real and imaginary parts of the refractive index $n = \eta + i\kappa = \sqrt{1+\chi}$ associated with the medium dispersion and absorption, respectively, are plotted in fig. 2 as a function of the probe detuning δ. The absorption vanishes at exact resonance and this is a striking result when compared with the situation in which the coupling field is absent ($\Omega_c = 0$) as this can make an otherwise completely opaque medium transparent to a resonant probe. As a consequence, a probe pulse in the EIT regime can propagate through the medium, but at a greatly reduced group velocity $v_g = (d\omega/dk) = c/(\eta + \omega d\eta/d\omega) << c$, due to the steep variation of $\eta(\omega_p)$.

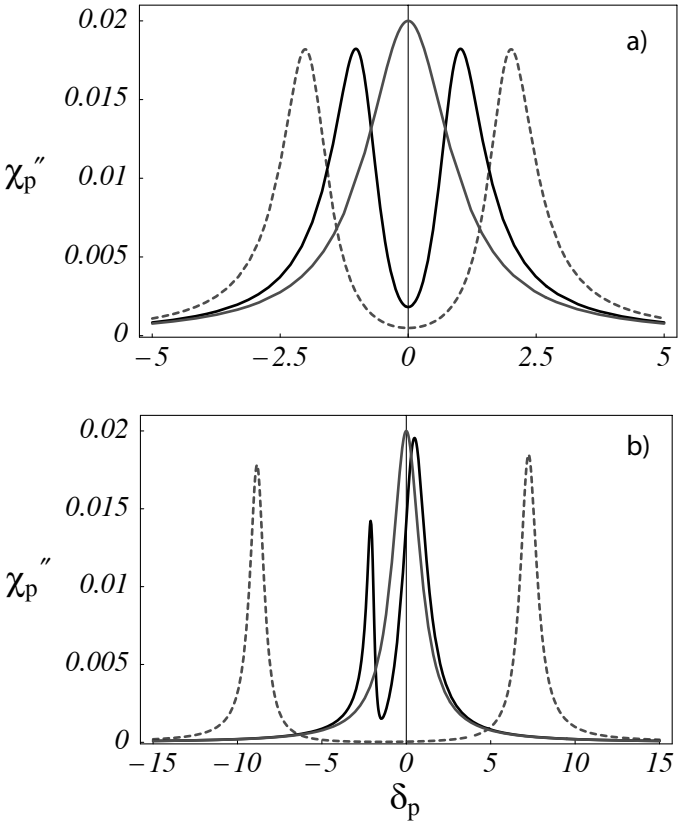

Fig. 3 Imaginary part of the susceptibility *vs.* the detuning δ_{eg} in units of γ. The upper and lower frame refer, respectively, to a resonant and non-resonant coupling beam with detuning $\delta_{em} = -1.6\,\gamma$. The coupling Rabi frequencies are (a) $\Omega_c/\gamma = 2$ (solid), 4 (grey dash) and (b) 2 (solid), 16 (grey dash). In the absence of the coupling beam the susceptibility is described by the solid grey curve [5].

3 EIT based on the yellow exciton levels in Cu_2O

A promising solid-state system for EIT has been identified in an undoped bulk semiconductor exhibiting sharp free-exciton lines that correspond to intrinsic delocalized electronic states . Specifically, we have considered [5] the "yellow exciton" series in Cu_2O for which an asymmetric lambda-type model Hamiltonian can be developed using the ground state of the crystal as state $|g\rangle$, a weakly allowed sublevel of the 2*P* exciton as state $|e\rangle$ and a forbidden 1*S* exciton sublevel as state $|m\rangle$, with the probe resonant frequency in the visible and the coupling resonant frequency in the infrared (see inset of fig. 4). For such a choice, all the relevant spectroscopic parameters are known and, thus, a realistic calculation can be made leading to a susceptibility of the same form as in eq. (1), where specifically γ =1 meV and $\gamma_{gm} = 0.1$ meV.
We show in fig. 3 both cases of a resonant and a non-resonant coupling: in the absence of the coupling beam the probe is absorbed (solid grey curve) while in its presence increasing degrees of transparency are observed to depend on increasing values of the pump beam intensity for a fixed detuning. The pump laser that couples the levels $|m\rangle$ and $|e\rangle$ splits the probe absorption line into two components each centered

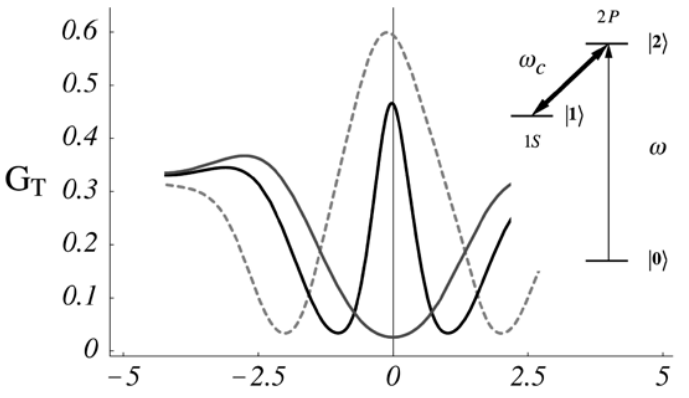

Fig. 4 Transmissivity G_T *vs.* the detuning δ_{eg} in units of γ; the background dielectric constant is $\varepsilon_b = 6.5 + i\,2\cdot 10^{-3}$. The coupling Rabi frequencies are $\Omega_c/\gamma = 2$ (black solid) and 4 (grey dash) while in the absence of the coupling beam the transmissivity is described by the solid grey curve [5].

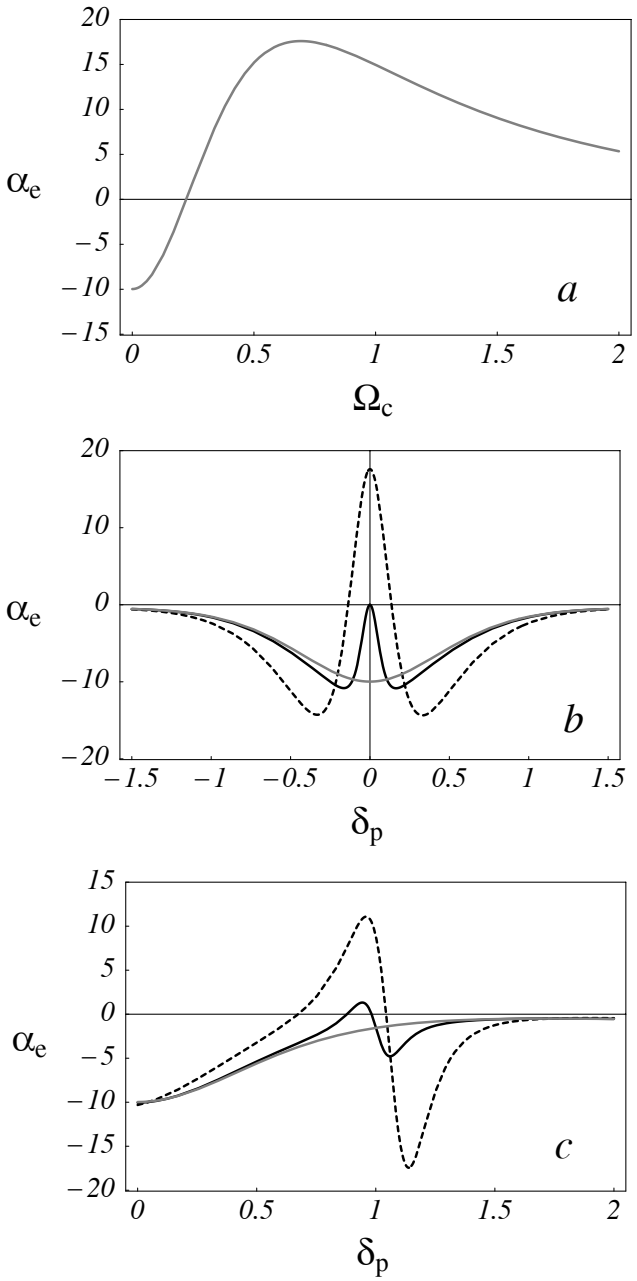

Fig. 5 Effective drag coefficient α_e *vs.* Rabi frequency Ω_c in units of γ for a resonant probe (a). Coefficient α_e *vs.* the detuning δ_{eg} for a coupling Rabi frequency $\Omega_c/\gamma = 0$ (grey), 0.18 (solid) and 0.7 (dash) for a resonant (b) and detuned (c) pump with $\delta_{em}/\gamma = 1$ [7].

at the transition frequencies from the ground state $|g\rangle$ to the two dressed excited states created by the coupling beam.These two components are separated by an amount that is equal to the ac Stark splitting $\Delta = \sqrt{(\Omega_c^2 + \delta_{em}^2)}$. For small Stark splittings, and roughly not exceeding twice the value of the dephasing γ of the ground to 2*P* transition, we observe a minimum in the absorption whenever the probe detuning equals that of the pump. The fact that the minimum occurs at the equal-detuning frequency, *i.e.* at the Raman resonance condition $\delta_{eg} = \delta_{em}$, is a manifestation of the induced coherence over the non-allowed transition between the ground and the 1*S* level. Under these conditions, such a reduction can be explained in terms of electromagnetically induced transparency as a combination of the Stark splitting and the destructive quantum interference between two different absorption paths from the ground state to the two dressed excited states. One could expect that (incoherent) bleaching or saturation effects would yield a similar absorption minimum; yet, these effects would be maximized for a probe close to resonance and not when it has the same detuning of the coupling beam. For large Stark splittings, on the other hand, the absorption is very small on the entire frequency range between the two well separated Autler-Townes sidebands. Such a uniform quenching does not originate from quantum interference because the upper doublet of dressed levels are now too far apart for the interference to take place.

The direct observation of induced transparency hinges on the actual transmission efficiency. We then consider the probe transmissivity G_T for a Cu_2O slab 35 μm thick at normal incidence, including an appropriate complex background dielectric constant, as shown in fig. 4. The quantum interference modifies the transmission linewidth in a non-trivial way, with the detunings and the coupling Rabi frequency being the free parameters to taylor the interference. In the absence of the pump, transmission would be quite small (G_T of the order of 10^{-2}) whereas when the coupling beam is on we can distinguish between two transparency regimes: one due to a large Stark splitting and the other due to quantum interference taking place, respectively, for strong- and weak-coupling intensities. For weak pumps, regardless of their detunings, the height of the transparency window increases appreciably more than its width does making the absorption to drop nearly 50%. The transmission linewidth can be subnatural ($< \gamma$) which is a typical feature of the electromagnetically induced transparency. Higher degrees of transparency are restrained more by the dephasing of the 1*S* to ground transition than by smaller thicknesses or higher coupling laser intensities; a smaller thickness would simply make the sample transparent altogether while higher pump-power densities would make the interference hard to achieve. On the other hand, by

reducing γ_{em} to half its value would produce a further 20% increase in the window height while its width would narrow down to nearly a third of γ. We stress in this respect that the value of $\gamma = 0.1$ meV used here is indeed rather conservative in view of recent experiments where a much narrower linewidth of the 1*S* exciton sublevels has been observed [6]. For sufficiently intense pumps, on the other hand, the transparency width increases more than the height does marking the transition to a large ac Stark splitting comprising a wide transparency band separated by two absorption dips in correspondence of the Autler-Townes sidebands.

4 Fresnel-Fizeau light drag and emission of Cherenkov radiation in the EIT regime

The slow light propagation characteristic of the EIT regime (see sect. 2) has a significant impact on many aspects of the electrodynamics of continous media. In particular, we have shown that two important effects such as the Fresnel-Fizeau light drag [7] and Cherenkov emission [8] could be qualitatively and quantitatively affected by the presence of the external coupling beam.

The phase velocity of light depends on whether light propagates in a moving or in a stationary medium. This effect, which gives rise to the familiar Fresnel light drag, has been observed for the first time in Fizeau's flowing water experiment and had a profound influence on the change of the perception of the nature of space and time corresponding to special relativity. Light drags can be made to vary over a rather wide range of values when a slab of coherently driven Cu_2O cuprous oxide is used as a dragging medium, due to the steep dispersion accompanying EIT. In particolar, in a typical interferometric experiment, the sensitivity at low drag velocities can be increased by at least one order of magnitude while having an appreciable transparency. On the other hand, one can also make the light drag to vanish over a broad range of probe frequencies depending on the pump parameters. This means that no fringe shift would be observed for light propagating through a moving medium with respect to light propagating through the same medium at rest.

The dragging medium, taken for instance in the form of a parallel-sided slab of thickness *L* moving at velocity *w*, induces an optical phase shift which can be cast in the form

$$\Delta\phi = \beta\alpha_e\,(\omega\, L/c) \tag{2}$$

where $\beta = w/c$ and α_e is the effective drag coefficient which depends on the dressed susceptibility of the medium [7]. We report in fig. 5 numerical results for a resonant as well as a detuned pump. Due to the high dispersion at the 2*P* exciton EIT resonance, where the absorption is quenched by quantum interference, large as well as vanishing drags are associated with an appreciable degree of transparency. At exact pump resonance, the effective drag coefficient reaches a very high value, whereas it vanishes for slightly detuned probes with a little smaller transparency.

A charged particle moving above a critical velocity in a dense medium emits an unusual type of radiation which was first observed in liquid media by Cherenkov and Vavilov, and later interpreted by Frank and Tamm. The study of such an effect was further extended to other condensed media where the emission of Cherenkov radiation turns out to be a very small fraction of the total energy lost by a fast charged particle. The loss of the incident particle energy is in fact mainly due to the ionization and to the excitation of the polarisable medium, however the Cherenkov contribution to the emitted radiation can be experimentally singled out from the particle total losses through the medium. In a resonant medium under the EIT regime, the external coupling field can qualitatively and quantitatively modify the energy loss of a fast charged particle due to Cherenkov emission [8]. Such effect can be described generalizing the theory of Cherenkov emission to the case of the dressed dielectric function appropriate for coherently driven Cu_2O as discussed above.

The first effect of the EIT regime is to select a narrow frequency range in which nearly resonant Cherenkov light can be efficiently emitted and then propagate with little absorption. As shown in fig. 6, this behaviour is prominent in coherently driven Cu_2O. The second effect is to modify the aperture θ of the cone on which the radiated energy is peaked (group cone) which in the EIT regime is much smaller than the aperture ϕ of the usual wave cone associated with

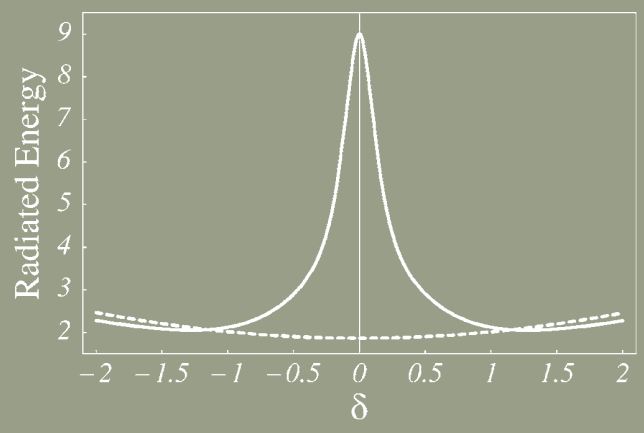

Fig. 6 Radiated energy in arbitrary units *vs.* the frequency detuning of the Cherenkov light in units of γ in the presence (solid) and in the absence (dash) of an external driving field. The charged particle velocity is $w = 0.9\,c$ and the coupling beam Rabi frequency is $\Omega_c/\gamma = 2$ (solid) [8].

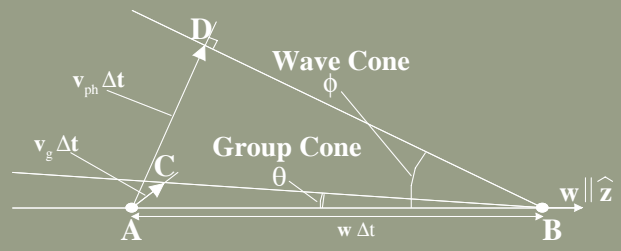

Fig. 7 Geometrical construction for the group cone. During the time Δt, the charge moves from A to B with velocity w , while the energy radiated in A propagates from A to C with a slow group velocity v_g.The straight line joining B and C is a generatrix of the group cone, while the line joining B and D is a generatrix of the wave cone determined by the phase velocity v_{ph} [8].

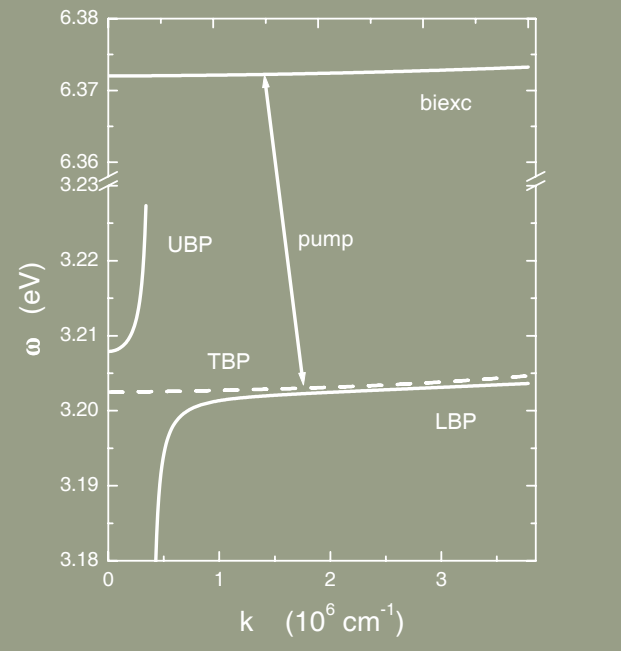

Fig. 8 Probe dispersion branches of coherently dressed CuCl. In the presence of the exciton-biexciton coupling pump, a third branch appears (dashed line) besides the usual upper and lower polariton ones. The frequency of the coupling beam is $\hbar\omega_c = 3.1695$ eV and its intensity corresponds to $\beta_c = 10^{-7}$ eV^2 [9].

the Cherenkov coherence condition which in isotropic, transparent non dispersive media is simply given by $\sin(\phi) = v_{ph}/w = 1/(n\,\beta)$. The effect is sketched in fig. 7 and it is simply due to the fact that the emitted Cherenkov light propagates with an ultraslow group velocity.

5 EIT based on exciton and biexciton levels in CuCl

Copper chloride (CuCl) is a prototype example of a semiconductor having an allowed interband transition and quite pronounced exciton and biexciton resonances. The conduction and valence bands of CuCl are parabolic and non-degenerate, with both extrema at the center of the Brillouin zone, opposite parities, and hole effective mass heavier than the electron one; as a consequence, exciton and biexciton in CuCl are a solid-state analogue of atomic and molecular hydrogen. Excitonic along with biexcitonic resonances may exhibit a variety of three-level configurations where EIT could in principle be achieved. In particular, a pump coherently driving the exciton-biexciton transition allows for a well-developed transparency within the exciton-polariton stop-band where a probe pulse may propagate, with a strongly reduced group velocity [9]. The large oscillator strength of the exciton-biexciton transition and the very narrow linewidth and long coherence time of the biexciton state with a small wave vector favor quite appreciable degrees of transparency. The phenomenon is similar to the EIT effects occurring in three-level atomic systems or in the forbidden yellow exciton in Cu_2O considered above, but the physics of the induced transparency within an otherwise reflecting stop-band relies here on a frequency and wave vector selective polaritonic mechanism [10], as in CuCl the one excitation eigenstates correspond to polariton states, *i.e.* coherent superpositions of the resonant exciton and photon states in the strong light-matter coupling regime. In fact, the Cu_2O exciton previously considered has a weak oscillator strength and hence negligible polaritonic effects making the basic physics underlying the phenomenon of EIT in that case much similar to the one occurring in atoms. Here, instead, the allowed exciton of CuCl exhibits a fully developed polaritonic stop-band and the delocalized nature of the intrinsic exciton-polariton or biexciton states having a well-defined wave vector k and a significant wave vector dispersion plays a crucial role, in strong contrast with the case of atomic levels having localized wave functions.

EIT can be induced in this case through a ladder scheme, in which a circularly polarized probe beam of frequency ω is nearly resonant with the transition from the crystal ground state to the exciton (having a parabolic dispersion $\omega_x(k) = \omega_T + \hbar k^2/(2\,m_x)$), while a pump beam having opposite circular polarization and frequency ω_c couples the exciton to the biexciton (having a parabolic dispersion

$\omega_m(k) = \omega_M + \hbar k^2/(2\, m_m)$). The CuCl response to a weak probe beam of frequency ω and wave vector **k**, in the presence of the strong coupling beam of frequency ω_c and wave vector $\mathbf{k}_c$ opposite to **k**, turns out to be described by the following dressed dielectric constant,

$$\varepsilon(k,\omega) = \varepsilon_b\,[1 + \Delta_{LT}/(\hbar\omega_x(k) - \hbar\omega - i\gamma_x + \Sigma)]\ , \quad \text{with}\ \ \Sigma = \beta_c/(\hbar\omega + \hbar\omega_c - \hbar\omega_m(k - k_c) + i\gamma_m)\ , \tag{3}$$

where Σ describes the nonlinearity due to the coherent pump and β_c is proportional to the pump intensity and the oscillator strength of the exciton-biexciton transition. All the CuCl material parameters appearing in eq. (3), *i.e.*, the exciton and biexciton $k = 0$ energies $\hbar\omega_T$ and $\hbar\omega_M$, their masses m_x and m_m and linewidths γ_x and γ_m, the background dielectric constant ε_b, and the exciton longitudinal-transverse splitting Δ_{LT} are known from experiment. The expression for ε in eq. (3) has the typical three-level EIT form (analogous to eq. (1), but here for a ladder scheme). When Maxwell's equations are solved with such dielectric constant in the absence of the pump ($\Sigma \to 0$) one obtains the usual upper and lower polariton dispersion branches and a polaritonic stop-band within which the probe is nearly completely reflected. The presence of the exciton-biexciton coupling through the pump introduces a third dispersion branch in the frequency region of the exciton resonance and this affects the probe transmission within the forbidden stop-band which can indeed be completely controlled. The relevant probe dispersion branches, obtained simply from the equation $c^2k^2/\omega^2 = \varepsilon(k,\omega)$ when all dampings are neglected are plotted in fig. 8 , showing in this case how the pump-induced new branch and the lower polariton branch anticross.
We show instead in fig. 9 the probe transmission spectra through a CuCl thin slab for different pump intensities and frequencies, with the inclusion of the exciton and biexciton dampings. A pronounced transparency window in correspondence of the pump-induced dispersion branch opens up within the polaritonic stop-band around a frequency $\omega = \omega_m(k - k_c) - \omega_c$, similarly to the usual EIT two-photon resonance condition. Unlike the exciton linewidth, the biexciton linewidth at a small wave vector γ_m results to condition the appearance of a transparency window, as expected in analogy with EIT in the ladder configuration in atomic systems. Differently from the case of EIT in atoms, the transparency frequency can be coherently controlled over a rather wide spectral range of several meV corresponding to the entire polaritonic stop-band. However, we remark that even within the transparency window the absorption is here still significant. Finally, we show in fig. 10 the delay experienced by a probe narrow Gaussian pulse propagating in the stop-band region of the coherently dressed thin slab. The pulse

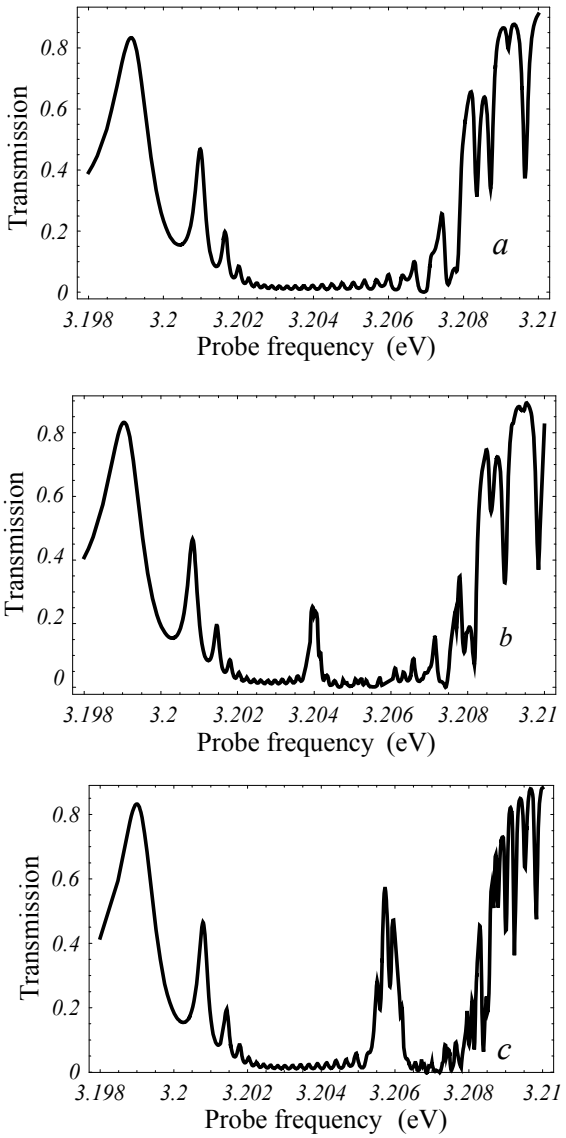

Fig. 9 Probe transmission spectra through a CuCl film 0.15 μm thick: a) no pump; b) with a pump of frequency $\hbar\omega_c$= 3.168 eV and intensity corresponding to $\beta_c = 5\cdot10^{-7}$ eV^2; c) with a pump of frequency $\hbar\omega_c$=3.166 eV and $\beta_c = 10^{-6}$ eV^2. The exciton and biexciton linewidths are γ_x= 50 μeV and γ_m = 15 μeV [9].

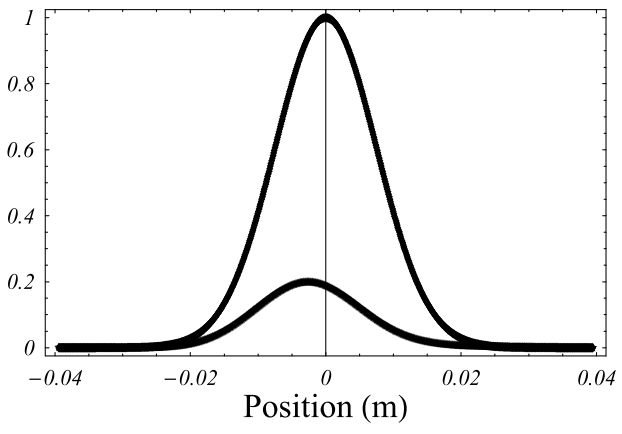

Fig. 10 Pulse profile in vacuum and after transmission within the transparency window induced by a pump of frequency $\hbar\omega_c$ = 3.168 eV and $\beta_c = 10^{-6}$ eV^2. The peak lag of 2.6 mm corresponds to $v_g = 5.8\cdot10^{-5}\,c$ [9].

is 20% transmitted across the stop-band, while from its delay one can infer a group velocity $v_g = 5.8 \cdot 10^{-5}\, c$. This turns out to be in good agreement with the slope of the third dispersion branch induced by the exciton-biexciton coupling and which most contributes to the pulse propagating within the sample. The pulse spatial length in the medium is expected to scale approximately with the ratio v_g / c with respect to its length in vacuum, and the remarkable spatial compression typically experienced by a pulse entering a slow-light medium [4] may also be observed in CuCl.

6 EIT-induced photonic crystals

In recent years, photonic band gap structures have been much investigated from the scientific as well as from the technological viewpoint [11]. Photonic crystals are inhomogeneous materials exhibiting periodic variations in space in one or more directions of their refractive index on length scales comparable to optical wavelengths. The periodic variation in their optical response leads to Bragg scattering of light and electromagnetic wave propagation becomes best described in terms of a photonic band structure, akin to the electronic band structure in a crystalline solid [12]. In particular, when the light wave vector is close to the Brillouin zone boundary the propagation of light is strongly affected, leading to the existence of a range of frequencies, known as a photonic band gap, for which light does not propagate. The periodic spatial dependence of the optical response in familiar photonic band gap materials and the corresponding photonic band structure are determined once and for all by the way the photonic crystal is grown. Yet, it would be of great interest the possibility to tune the photonic confinement by optical means which can be efficiently done by using a modified standing wave EIT configuration amenable to be implemented in atomic samples as well as in nitrogen-vacancy color centers in diamond [13]. In this case, the periodic modulation of the optical response is directly created via all-optical nonlinearities, while the underlying material medium is homogeneous, and the photonic band structure is fully determined, rather than just modified, by one or more control beams.

An efficient mechanism to achieve very large modulations of the optical properties relies on quantum coherence and interference in multilevel systems, the simplest of which is a three-level atom in a lambda configuration commonly used to observe EIT with a monochromatic control beam (see fig. 1). When travelling waves are used as control beams, the dressed dielectric function experienced by a weak probe beam does not vary in space, yet when a standing wave configuration for the pump is employed, the probe optical response is modulated periodically in space realizing a photonic band gap system. This amounts to the use in eq. (1) of a space dependent Rabi frequency of the form

$$(4) \quad \Omega_c^2(z)/\Omega_o^2 = (1 + R_m)^2 \cos^2(\pi z / a) + (1 - R_m)^2 \sin^2(\pi z / a)$$

corresponding to a configuration obtained retroreflecting a beam of Rabi frequency Ω_o on a mirror of reflectivity R_m, and its spatial periodicity is half the control beam wavelength $a = \lambda_c / 2$. It is also of interest a configuration in which the forward and backward control beams are slightly misaligned by an angle θ, in which case the spatial periodicity given by $a = \lambda_c / (2 \cos(\theta/2))$ can be moderately tuned. For a perfect standing wave $R_m = 1$ and the pump intensity vanishes at the nodal positions around which the medium remains normally absorbing. Yet, it is sufficient to reduce the reflectivity of the mirror to make the pump intensity nowhere vanishing with nodes becoming quasi-nodes.The probe thus progates in the coherently dressed system as in a one-dimensional photonic crystal and, because in a symmetric lambda configuration the probe frequency is close to the coupling frequency, the probe wave vector is close to the corresponding Brillouin zone boundary π/a where a photonic stop band is expected to open.

While cold alkali atoms are excellent candidates to implement such a scheme, for many potential applications solid-state solutions would be preferred owing to obvious advantages: high atomic densities, absence of atomic diffusion, compactness, simplicity of operation and scalability just to mention a few. Color centers in diamond, in particular, have attracted over the past few years a renewed interest for their potential as single-photon sources and quantum memories in solids. The N-V color centers are attractive as they behaves a bit like a multilevel atom trapped in the diamond lattice. Composed of a substitutional nitrogen next to a carbon vacancy, these centers can have extremely long-lived spin coherence. In addition, they also have interesting optical properties as they exhibit a configuration with two ground state levels connected to a common excited state by optical transitions of moderate strength leading to a symmetric lambda-type level configuration amenable to the observation of EIT effects, and to the implementation of the above scheme for all-optical photonic crystals provided the inhomogeneous broadening of the color center levels is properly accounted for.

We now proceed to illustrate how pulse propagation in N-V diamond color center samples may be all-optically controlled via a modified standing way EIT configuration. We adopt here realistic parameters as taken from recent experiments on coherent population trapping in N-V color centers, in particular, using as inhomogeneous linewidths

of the e-g and m-g transitions the values $\Gamma_{eg} = 375$ GHz and $\Gamma_{mg} = 2.5$ MHz, respectively. The inhomogeneous broadening can either be taken into account analytically using a Lorentzian lineshape or, more realistically, by numerically integrating over a Gaussian profile. Owing to the unphysically long tails of a Lorentzian broadening distribution, the corresponding EIT window turns out to be shallower than the one obtained by using a Gaussian inhomogeneous broadening profile. In the latter case, the low values of residual absorption in the EIT region are in turn responsible for the well-developed photonic band-gap structure shown in fig. 11. The gap is characterized as the frequency range (roughly from 0 to 20 MHz) in which Re $(k) = \pi/a$ and Im $(k) \neq 0$, while in the bands Im $(k) \approx 0$. Correspondingly, probes with frequencies inside the bandgap will experience almost perfect reflection (over 99 %) for a sample of finite length as shown in fig. 12(a). The width and position of the stop band can be controlled by changing the misalignment angle θ and the Rabi frequency Ω_o. The reflection and transmission spectra in fig.12 (a) and (b) display, in addition, rapid oscillations (fringes) near the bandgap due to the interference arising from the front and back surfaces of the sample. The presence of fringes, however, is tightly related to the background absorption. When this is included in the expression of the refractive index used to evaluate the spectra as in fig.12 (a) and (b) (dotted curves), it can in fact well smooth out the oscillations yet maintaining high values of the reflectivity. In fig. 13, we show the reflected and transmitted probe pulse intensities.When all frequency components of the probe are inside the bandgap (see fig. 13 (d)), the reflected pulse has essentially no loss or deformation. Conversely, the reflected pulse is increasingly suppressed and distorted as the probe frequency carrier gradually moves away from the center of the stop band, and, simultaneously, a stronger transmitted pulse is observed. Such a controllable stop-band

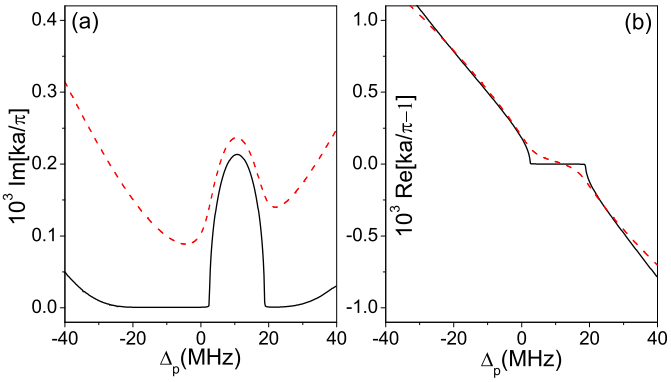

Fig. 11 N-V diamond photonic band-gap near the first Brillouin zone boundary induced by a standing-wave coupling field with $\Omega_o = 20.0$ GHz, $R_m = 0.62$, and $\theta = 38$ mrad. Solid and dashed curves refer, respectively, to an inhomogeneous Gaussian and Lorentzian broadening profile [13].

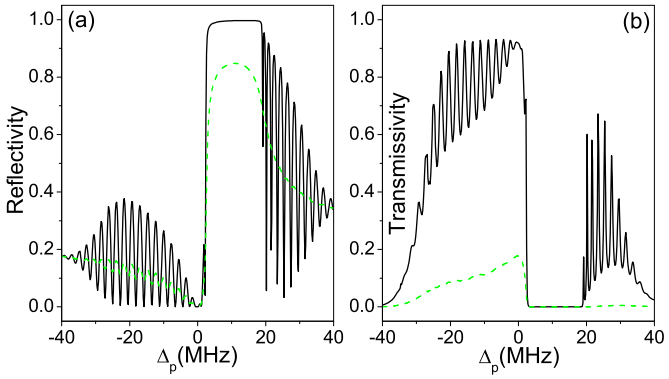

Fig. 12 Probe reflectivity and transmissivity spectra for a 2.0 mm long N-V diamond sample. The green-dashed curves correspond to a background absorption of Im $\varepsilon_b = 0.0002$, which is an illustrative value much larger than the actual one. The standing-wave driving field parameters are the same as those in fig. 11 [13].

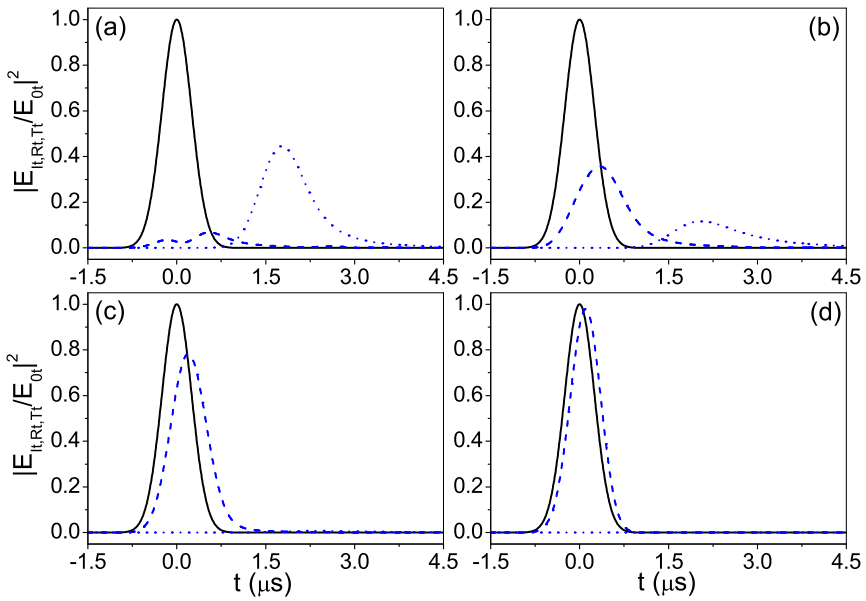

Fig. 13 Pulse dynamics of an incident (black-solid) probe impinging upon a 2.0 mm long N-V diamond sample. The parameters of the standing-wave coupling field again are the same as those in fig. 11 while the reflected (blue-dashed) and transmitted (blue-dotted) intensities are scaled to the incident probe pulse peak intensity. The frequency width of the incident pulse is 4.0 MHz and the detunings of its frequency carrier are, respectively, (a) 0.0 MHz; (b) 3.0 MHz; (c) 6.0 MHz; (d) 10.0 MHz [13].

mechanism may easily be exploited to devise an all-optical dynamically tunable beam-splitter for applications in light storage and quantum communication processing.

Acknowledgements

It is a pleasure to thank the many colleagues who have collaborated with us on EIT-related problems, and particularly I. Carusotto, S. Chesi, A. Mysyrowicz and J.-H. Wu.
This contribution is dedicated to the memory of Franco Bassani, an extraordinary man, teacher and leader who has recently passed away. He has been definitely the driving force in most of the ideas reviewed here, and he will be missed as a scientist and by all of us who looked upon him for inspiration and guidance over the years.
Financial support from the MIUR (PRIN 2006 - grant 021037 and Italy-Spain Azione Integrata - grant IT09L244H5) and the CRUI-British Council exchange grant is gratefully acknowledged.

References

[1] M. Scully, M. Zubairy, "*Quantum Optics*" (Cambridge University Press, Cambridge) 1997.
[2] S. E. Harris, "*Electromagnetically induced transparency* ", *Phys. Today,* 50 no. 7 (1997) 36.
[3] E. Arimondo, "*Coherent population trapping in laser spectroscopy*", in *Progress in Optics XXXV,* edited by E. Wolf (Elsevier, Amsterdam) 1996, p. 257.
[4] M. Fleischhauer, A. Imamoglu, J. P. Marangos, "*Electromagnetically induced transparency: Optics in coherent media*", *Rev. Mod. Phys*., 77 (2005) 633.
[5] M. Artoni, G. C. La Rocca, F. Bassani, "*Electromagnetic-induced transparency of Wannier-Mott excitons*", *Europhys. Lett.,* 49 (2000) 445.
[6] K. Yoshioka, M. Kuwata-Gonokami, "*Dark excitons in Cu_2O crystals for two-photon coherence storage in semiconductors*", *Phys. Rev. B,* 73 (2006) 081202.
[7] M. Artoni, I. Carusotto, G. C. La Rocca, F. Bassani, "*Fresnel light-drag in a coherently driven moving medium*", *Phys. Rev. Lett*., 86 (2001) 2549; I. Carusotto, M. Artoni, G. C. La Rocca, F. Bassani, "*Transverse Fresnel-Fizeau drag effects in strongly dispersive media*", *Phys. Rev. A* 68 (2003) 63819.
[8] I. Carusotto, M. Artoni, G. C. La Rocca, F. Bassani, "*Slow group velocity and Cherenkov radiation*", *Phys. Rev. Lett*., 87 (2001) 64801; M. Artoni, I. Carusotto, G. C. La Rocca, F. Bassani, "*Vavilov-Cherenkov effect in a driven resonant medium*", *Phys. Rev. E,* 67 (2003) 46609.
[9] S. Chesi, M. Artoni, G. C. La Rocca, F. Bassani, A. Mysyrowicz, "*Polaritonic stop-band transparency via exciton-biexciton coupling in CuCl*", *Phys. Rev. Lett*., 91 (2003) 57402; F. Bassani, G. C. La Rocca, M. Artoni, "*Electromagnetically induced transparency in bulk and microcavity semiconductors*", *J. Lumin*., 110 (2004) 174.
[10] V. M. Agranovich, V. L. Ginzburg, "*Crystal Optics with Spatial Dispersion and Excitons*" (Springer, Berlin) 1984.
[11] S. Johnson, J. Joannopoulos, R. Meade, J. Winn, "*Photonic Crystals: The Road from Theory to Practice*" (Kluver, Norwell) 2002.
[12] F. Bassani, G. Pastori Parravicini, "*Electronic States and Optical Transitions in Solids*" (Pergamon Press, Oxford) 1975.
[13] M. Artoni, G. C. La Rocca, "*All-optical tunable photonic band gaps*", *Phys. Rev. Lett*., 96 (2006) 073905; J.-H. Wu, G. C. La Rocca, M. Artoni, "*Controlled light-pulse propagation in driven color centers in diamond*", *Phys. Rev. B,* 77 (2008) 113106; J.-H. Wu, M. Artoni, and G. C. La Rocca, "*Controlling the photonic band structure of optically driven cold atoms*", *J. Opt. Soc. Am. B,* 25 (2008) 1840.

Giuseppe La Rocca

Giuseppe La Rocca after his studies at the University of Pisa and Scuola Normale Superiore, and later at Purdue University (Usa), has been Alexander von Humboldt research fellow at the Max-Planck-Institut für Festkörperforschung (Germany), research associate at Scuola Normale Superiore and associate professor at the University of Salerno. Since 2001, he is associate professor of solid-state physics at Scuola Normale Superiore. His main research interests are in condensed-matter theory, particularly the electronic states and optical transitions in solids. His recent activities concern the linear and nonlinear optics in organic semiconductor microcavities, the physics of hybrid organic-inorganic nanostructures, the spin-orbit coupling effects in semiconductors and the coherent control of light-matter interaction.